Development 99, 187-196 (1987)
Printed in Great Britain © The Company of Biologists Limited 1987

A probabilistic model of mosaicism based on the histological analysis of chimaeric rat liver

P. M. IANNACCONE*, W. C. WEINBERG and L. BERKWITS

Department of Pathology and Northwestern University Cancer Center, Northwestern University Medical School, 303 E.Chicago Ave., Chicago, IL 60611, USA

* To whom correspondence should be addressed

Summary

The analysis of pattern development in mosaic and chimaeric animals has provided insight into a number of developmental problems. In order to aid the understanding of the dynamics of the development of mosaic tissues, a computer simulation of the generation of a mosaic tissue was created using simple probabilistic decisions. Results of quantitative analysis of the simulated mosaicism were compared with chimaeric liver. Chimaeric animals were produced by morula aggregation between histologically distinguishable strains of congenic rats. The livers of these animals revealed a pattern of patchy mosaicism unrelated to either acinar or lobular architecture of the organ. Independent quantifiable parameters were correlated and compared between the simulation and chimaeric liver tissue. This analysis showed that extensive cell migration is not required to develop finely variegated mosaic tissue and that the patterns of mosaicism observed could have resulted from tissue development in which as few as three reiterated decisions were required. First, the simulation established anlagen of two cell types of various specified proportions with randomly chosen placement. Second, in each generation of the simulation the order in which the cells divided was established randomly. Third, there was a random choice of the direction of placement of the daughter cell. The quantitative relationships between the proportion of cell types, the area of patches and the number of patches per unit area was consistent between the simulation and the chimaeric tissue.

Key words: rat liver, chimaera, pattern formation, mosaic tissues, computer simulation.

Introduction

Chimaeric animals, produced by the amalgamation of zygotes with subsequent development in surrogate mothers, have been used to establish the patch size and coherent clone size of solid viscera in order to deduce mechanisms of organogenesis (Iannaccone, 1980; West, 1975, 1976; Hutchison, 1973; Lewis, 1973). This approach has been limited by the lack of histological markers that are capable of distinguishing closely related strains of inbred animals. Such markers are necessary for the analysis of organ development in chimaeras whose embryonic cellular assortment is not influenced by disparate genotype combinations. Another limitation has been the lack of suitable quantitative methodologies that facilitate such analysis. Where appropriate methodologies were available, models of mosaicism were developed to support theories concerning the generation of such tissues (West, 1975, 1976; Whitten, 1978; Hutchison, 1973). Previous models of mosaicism have mainly examined the relationship between the proportion of cell types present in the mosaic tissue and clone size as well as distribution of the cell lineages present in the mosaic tissue. None of the models described to date deal with the generation of the mosaic tissue.

Investigation of the degree of tissue variegation in the liver has led to conflicting conclusions concerning the degree of clonal expansion of primordial elements in the liver. Studies based on the observation of variation in proportion of isoenzyme activity in large numbers of small samples indicated that the liver had large contiguous areas of similar lineage, and thus little cell migration had occurred in the development of the organ (Wegmann, 1970). When this tissue was reexamined with histological markers of mosaicism,

β-glucuronidase or ornithine carbamoyltransferase, it was apparent that there was far less clonal expansion than previously expected (West, 1976; Wareham, Howell, Williams & Williams, 1983). These studies led to the conclusion that a high degree of variegation meant that active cell migration occurred late into development and resulted in relatively little coherent clonal expansion.

For this report mosaic liver tissue was analysed in chimaeric rats made between congenic strains in which the mosaicism could be demonstrated histologically using a system in which the lineage of cells comprising most visceral organs could be established (Weinberg, Howard & Iannaccone, 1985*b*). Patterns of mosaicism were discerned and analysed quantitatively utilizing monoclonal antibodies against class I antigens which vary between the strains used to construct the chimaeras. We describe a computer simulation of the generation of mosaic tissue in order to test several assumptions concerning the formation of mosaic liver. The simulation was programmed to begin with an anlage of a specified proportion of two cell types randomly distributed. In each generation all cells divide in a random order and the daughter cells occupy an adjacent position chosen randomly. The comparison of the computer simulation with chimaeric tissue revealed that extensive cell migration is not required for fine variegation of mosaic tissue and that such tissue patterns can arise as the result of a few, highly reiterated, simple decisions.

Materials and methods

Chimaera production

Chimaeras were produced by the amalgamation of embryos of PVG strain congenic rats. The rats were maintained by sib mating in a facility with constant temperature and humidity. The light cycle was reversed to facilitate the timed removal of embryos. Mating was determined to have occurred by observing sperm in the vaginal smear; the day of discovery was considered day 0 of the pregnancy. Oviducts of pregnant females of the appropriate strains of animals were flushed on day 3 of pregnancy with a phosphate-buffered medium (Papaioannou & West, 1981) using a 30-gauge stainless steel needle. Zonae pellucidae were removed by brief treatment with acid tyrode containing polyvinylpyrolidine (Nicolson, Yanagimachi & Yanagimachi, 1975). Zona-free morulae were apposed in microdrops of Bigger's media supplemented with vitamins as previously described (Yamamura & Markert, 1981). The amalgamated embryos were held for several hours in a 5 % CO_2 atmosphere at 37°C. The morulae pairs were then moved to a CO_2 incubator and cultured overnight. The following afternoon the pairs that had successfully mixed were transferred to the uteri of pseudopregnant Holtzman rats. The surrogates were used on day 3 of pseudopregnancy following mating with vasectomized male Holtzman rats. Mating was determined to have occurred by discovery of a copulatory plug (day 0 of pseudopregnancy).

Genotype marker

The congenic PVG rats vary in the expression of class I antigens that can be recognized by a variety of monoclonal antibodies directed to these *RT1* differences. The strains used in this study have been designated PVG-*RT1*^{a} and PVG. The antibodies were obtained from Dr J. C. Howard (Cambridge, UK). The use of these antibodies to distinguish the tissues of the congenic strains has been described previously (Weinberg, Deamant & Iannaccone, 1985*a*). Briefly, the monoclonal antibodies were iodinated by 30 s nondestructive treatment with chloramine T. The iodinated monoclonal antibody was applied to fresh cryostat sections of tissue which had been incubated with PBS containing 10 % fetal calf serum and 10 % nonimmune PVG-*RT1*^{u} serum for 30 min at 4°C. The tissue sections were then incubated with iodinated monoclonal antibody for 1 h at 4°C. The sections were rinsed in PBS containing 10 % FCS, washed extensively in cold PBS, fixed and dried.

Autoradiography

The labelled sections were coated with NTB-2 photographic emulsion (Kodak, Rochester, NY) at 42°C. The slides were dried in the dark with ambient conditions for 2–3 h, then stored in the dark at 4°C for 3–5 days. At the end of this exposure time the slides were developed in D-19 developer (Kodak, Rochester, NY) diluted 1:1 (v/v) with water, rinsed in dilute acetic acid and fixed with Kodak fixative.

Photography

The autoradiograms were photographed with a Leitz epivert microscope using Kodak EPY-50 emulsion.

Computer simulation of mosaic tissue growth

The tissue was modelled with a two-dimensional tablet of numbers containing 76 vertical positions and 76 horizontal positions. Each element of this matrix represented a cell within the tissue. The elements assumed one of three values. Zero denoted unoccupied elements. A value of one denoted the presence of a cell of type 1, while a value of two denoted a cell of type 2. The 100-cell 'anlage' consisted of cells of types 1 and 2 in a proportion that was approximately specified. The precise proportion of the cell types varied slightly by chance. The distribution of type 1 and type 2 cells was random.

Division of cells in the matrix was accomplished by choosing the direction in which the 'daughter cell' moves following division, then selecting which cell divides. Cells may divide in eight possible directions with respect to the parent cell. If the direction of the neighbouring element directly above the parent cell was called 0°, then a cell may divide in the following directions: 0°, 45°, 90°, 135°, 180°, 225°, 270° and 315° (Fig. 1). All cells within the matrix were assigned a direction of division in a random fashion. This direction was stored in the same element of the matrix that contained the cell type. Each element was then selected at random. The cell was divided in the division direction

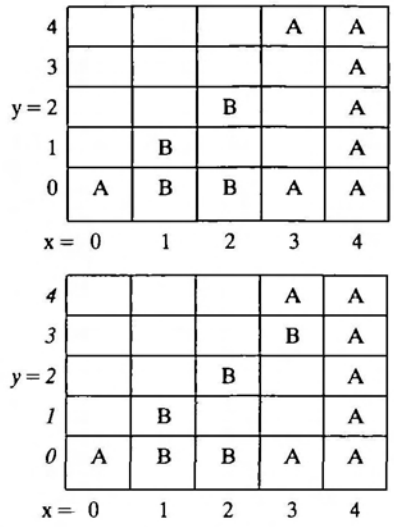

Fig. 1. Division of parent cell at x = 2, y = 2 in the 45° direction. Daughter cell is produced at x = 3, y = 3.

previously chosen. When cells have divided, the neighbouring cells must be shuffled in the direction of division to accommodate the newly formed daughter cell. If a nonoccupied element was present in the direction of division, the cells were shuffled up to the nonoccupied element. In this manner, the 'tissue' expanded to fill the vacant space within the matrix. When all of the elements had divided, one 'generation' was completed (Fig. 2).

The simulation was performed at specified starting proportions (pr) of type 1 cells of 0·5, 0·6, 0·7, 0·8 and 0·9. The simulation completed three independent runs of ten generations each. The actual proportions varied with each run and the average proportions tested were 0·537 (±0·002), 0·650 (±0·023), 0·706 (±0·019), 0·793 (0·030) and 0·92 (±0·007). Quantitative determinations were made for each run at each specified proportion and at each generation. The determinations were made as described below and included the number of patches per unit area (number of patches in the total area of the matrix with occupied elements at a given generation) of simulated tissue, the average area (number of contiguous occupied elements of a given type) of the patch, and the actual proportion of the two 'cell' types in the simulated tissue. A second simulation of three independent runs with specified proportions of type 1 cells of 0·1, 0·2, 0·3, 0·4, 0·5 was performed to demonstrate that the results of the simulation were not biased by which proportions were chosen to start the simulation. The actual proportions run were type 1 cells = 0·10 (±0·01), 0·17 (±0·003), 0·31 (±0·014), 0·38 (±0·015), and 0·49 (±0·03).

Analysis of the regions of contiguously similar cell type (patches) employed the image-processing techniques of feature extraction and region labelling. The features of type 1 and type 2 tissues were extracted from the matrix and a component labelling algorithm (modified from Rosenfeld & Kak, 1976) was applied to the extracted features. Once the labelling was completed, the number of regions and the area of each labelled region in the tissue were determined. A mean and standard error of these areas were computed. Regions that included elements along the border of the matrix were not included in the computation of mean and standard error of areas. Border regions were included in the determination of number of regions. Growth of mosaic tissue was simulated on an NEC-APC 16-bit microcomputer (8086) with 128 K of memory. The simulation software was written in the C language and compiled with the Aztec C compiler. The application ran under the CP/M-86 operating system.

Digital quantification

The photomicrographs were projected onto a digitizing tablet (Summagraphics MM1200) through a first surface mirror. The patches were then traced with the tablet cursor and percent parental genotype, number of patches/unit area and average patch area were computed using a microcomputer and a program previously described in detail (Berkwits & Iannaccone, 1985). The smallest patch digitized by this method was 80 μm^2 in area representing a single hepatocyte. Patches consisting of 2–10 hepatocytes were easily digitized by this method.

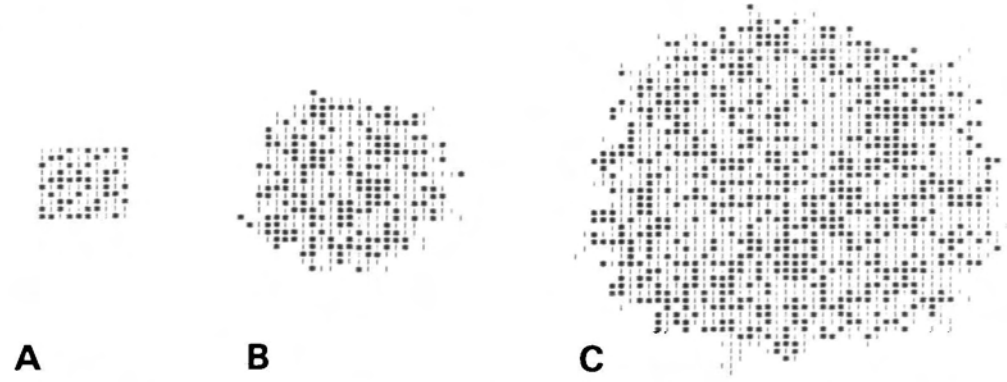

Fig. 2. Representation of the computer-generated mosaic tissue. A represents the starting 'anlage' at generation 0. The proportion of the two 'cell' types, # and −, was selected as described in 'Materials and methods'. B represents generation 2 and C represents generation 4 produced by the stimulation as described in 'Materials and methods'.

Statistical evaluation

All of the relationships presented in this report were established statistically using Pearson's moment–product correlation test to establish a coefficient of correlation (r). The significance of the linear association is presented as the probability that the association occurred by chance alone (P). This probability was established using a t-test of the coefficient of correlation for degrees of freedom less than 30 (Bruning & Kintz, 1968). The standard errors of the means are presented.

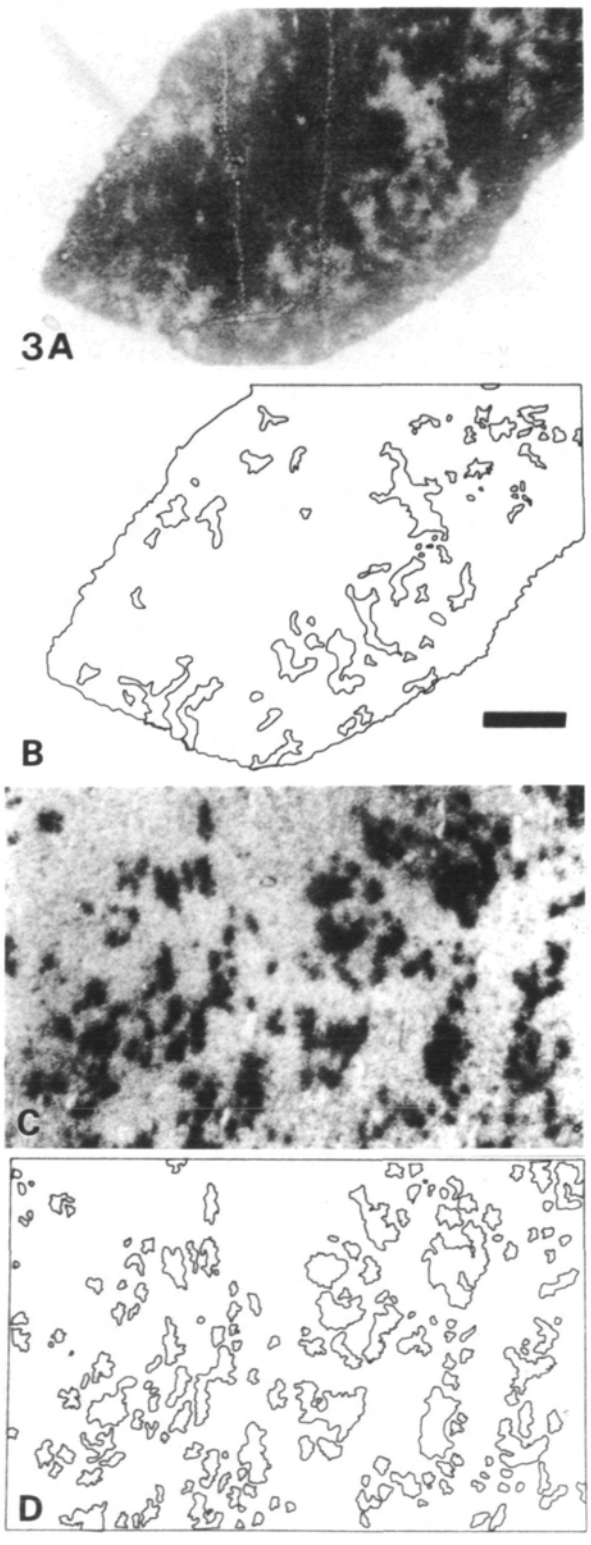

Results

Liver tissue from the two parental strains of rat demonstrated uniform presence or absence of grain accumulation in the autoradiograms appropriate to the genotype under consideration (Weinberg *et al.* 1985*a*). Sections of liver from all of the chimaeric animals, however, demonstrated patchy mosaicism as shown in Fig. 3. Fig. 3 also demonstrates a typical digitized section of the chimaeric livers. These plots represent the reconstruction of digitized data and were used in all cases to check the accuracy of the digitization of sections. The patches (contiguous regions of the same lineage) were randomly placed in the tissue with no apparent relationships to the distribution of liver structures. There was no evidence of zonal distribution of mosaicism in any of the animals. The comparison of sections demonstrating patch distribution with serial haematoxylin- and eosin-stained sections (Fig. 4) failed to demonstrate an association between patches and either the lobular architecture or the acinar architecture of the liver.

The randomness of the patch in the liver with reference to the microscopic or functional anatomy of the organ led to the supposition that the organogenesis of the liver requires relatively simple decisions. This hypothesis was tested by creating a computer simulation of the formation of a mosaic tissue in two dimensions by reiterating simple decisions (randomly distributing cells in an anlage, randomly choosing the order of division during each generation and randomly choosing the adjacent position of the daughter). The simulated tissue was analysed at each generation. The number of patches per unit area was determined to be nearly equal at equal proportions of the two cell types, $pr = 0{\cdot}53$, in all generations. The number of patches of the minor cell type, however, increased rapidly as a function of generation number at $pr > 0{\cdot}65$ (Fig. 5). This relationship reflects the formation of a lattice of the major cell type at relatively low proportions. By $pr > 0{\cdot}79$ there is a

Fig. 3. (A) Unstained autoradiogram of section 11 of the liver of animal 0906. The image was digitized as described in 'Materials and methods' for quantitative analysis and the digitized section, as seen by the computer, is shown in B. This section represents an animal with a larger proportion of PVG-*RT1*^{a} derived cells, thus patches of PVG were traced. (C) An unstained autoradiogram of section 18 from the liver of animal 0912. (D) The digitized data from this section in which patches of the PVG-*RT1*^{a} type were analysed. The photomicrographs (A,C) are ×45; in the digitized sections (B,D) bar, 0·25 mm.

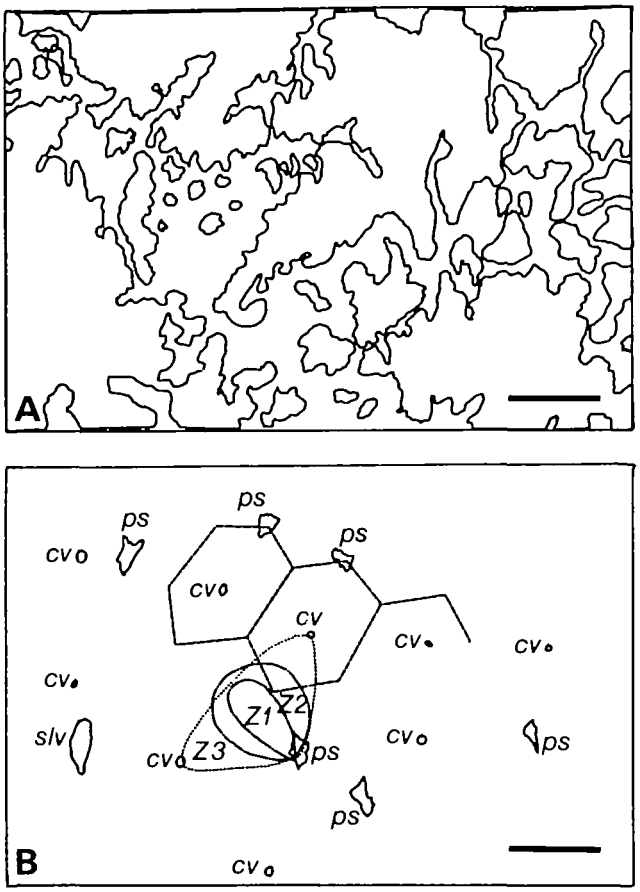

Fig. 4. Computer-generated plots of digital data from liver sections of animal 0911. (A) Data from an unstained autoradiogram of liver section 1, showing the distribution of patches of PVG-*RT1*^{a} lineage. Since the proportion of cells of this lineage was less than 0·7 (pr = 0·66) it was possible in this instance to trace the PVG-*RT1*^{a} patches. (B) A serial frozen section was stained with haematoxylin and eosin (H&E) and pin registered to the autoradiogram (i.e. the sections were aligned using independent registration marks in the tissue of each section to ensure that there was no bias in their reconstruction). Several liver lobules are outlined (– – –). The liver lobule is roughly hexagonal in cut section and is defined by portal triad spaces (*ps*) and with a central vein (*cv*) in the middle of the lobule. Liver cell plates (not shown) radiate toward the *cv*. The liver acinus, on the other hand, is arranged around a circulatory tree defined by the terminal hepatic arteriole. An example of a liver acinus is outlined (. . .). *Z1*, *Z2*, and *Z3* refer to zones of progressively poorer quality arterial blood supply. A sublobular vein (*slv*) is present. The liver lobule and the liver acinus represent the two predominant current views of anatomic organization in the liver. There is no apparent relationship between the distribution of patches and either lobular or acinar architecture in any of the sections examined. Bar, 0·25 mm.

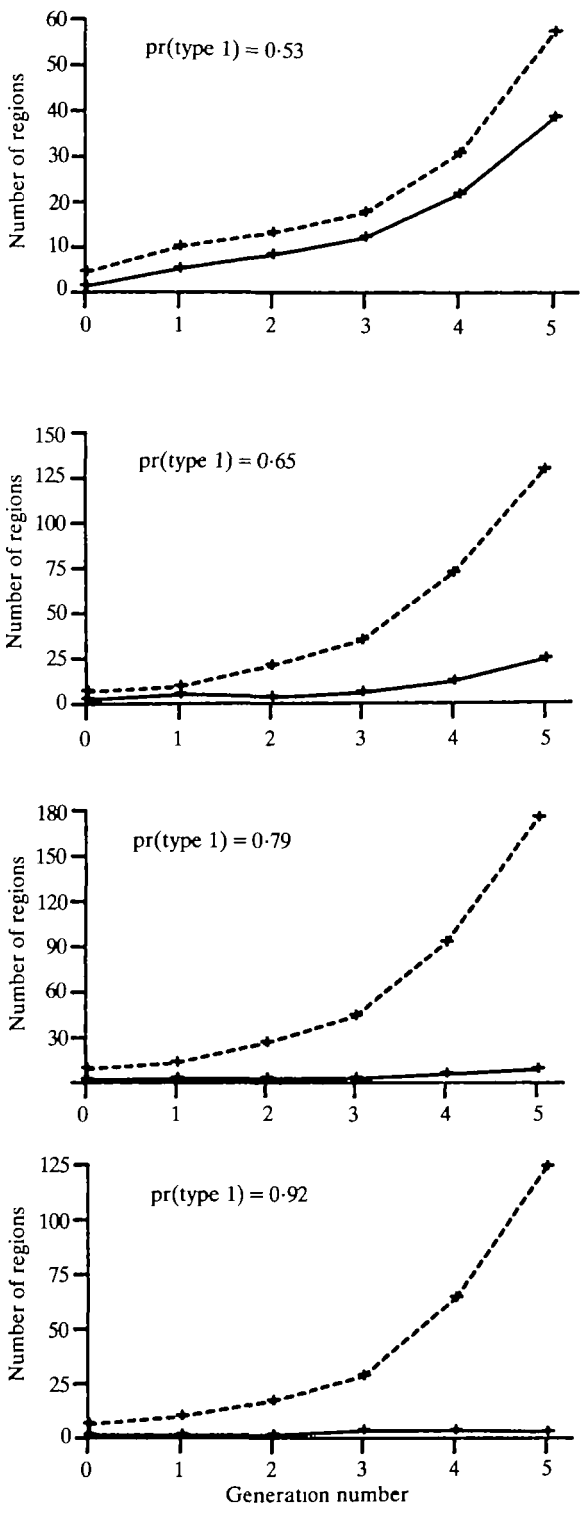

Fig. 5. The relationship between the number of regions in computer-simulated mosaic tissue and the generation number of the tissue. This relationship is presented for four preparations (pr) of type 1 cells in the initial 'anlage' as described in 'Materials and methods'. The solid lines represent type 1 regions and the dashed lines represent type 2 regions. As described in 'Results' the number of regions of the major type (type 1) approaches 1 (a lattice) at proportions in excess of 0·7.

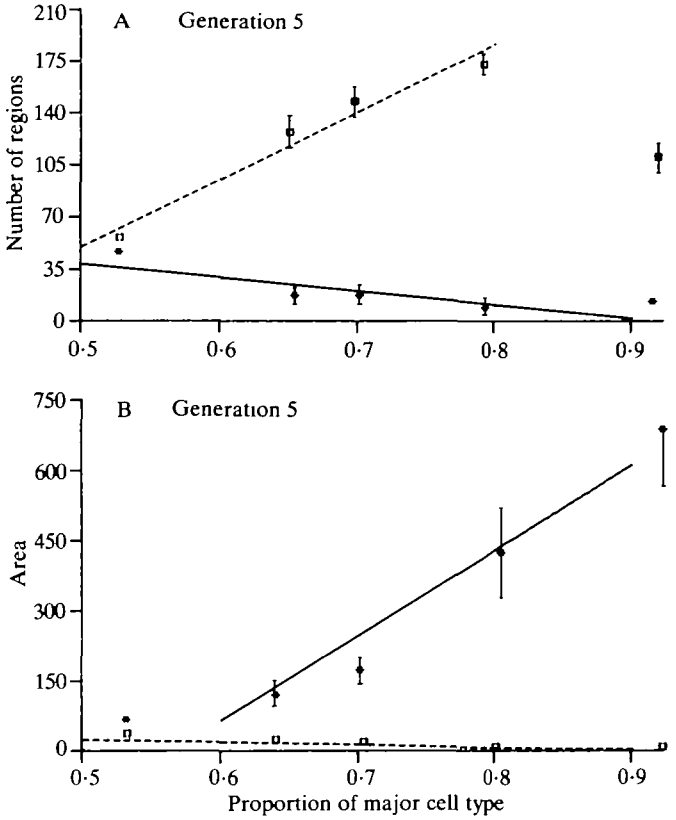

Fig. 6. The correlation between the number of regions (patches) per unit area (A) and the area (in arbitrary units) of regions (B) in the computer-simulated mosaic tissue and the proportion of type 1 cells (major type) in the 'tissue' at generation 5. Since the computer uses algorithms that can analyse the background lattice as well as the minor 'cell' type, this correlation is presented for both 'cell' types as a function of type 1 proportion. The dashed line represents type 2 (minor type) regions and the solid line represents type 1 (major type) regions. As described in 'Results', the number of type 2 regions (minor type) increases rapidly as the probability of the type 1 cells (major type) increases up to a proportion of approximately 0·8. Standard errors of the means (S.E.M.) are presented as vertical bars unless the S.E.M. bar is smaller than the symbol representing the mean.

background lattice in the first generations and only after three generations does the number of patches begin to rise as this lattice is fragmented. By pr > 0·92 the number of major cell type patches was essentially invariant with generation. The number of patches/unit area was examined as a function of the proportion of the major cell type at generation five. Five generations were sufficient to bring the developing 'tissue' to the limit of the image analysable matrix. The relation between pr and the number of regions (patches) per unit area is shown in Fig. 6. The number of type 1 regions between pr values of 0·5 and 0·9 decreases with a shallow negative slope. The two parameters fit a linear model with a correlation coefficient of −0·97 ($P < 0·001$). As in chimaeric liver tissue (below), the number of patches of the minor type per unit area increased as a linear function of pr ($r = 0·98$; $P < 0·001$).

The computer-simulated data cannot generate absolute areas with any meaning biologically; however, arbitrary area units can be used to determine the extent of correlation between the proportion of a given cell type and patch area at any generation selected (Fig. 6). The computer model and liver sections from the chimaeras (Fig. 7) displayed similar correlations between these two independently quantifiable parameters. From these data it is clear that as the proportion of a given cell type increases the area of patches generated by that cell type increases. This is the inverse of the relationship between proportion and number of patches per unit area.

The plausibility of this model could be tested by comparing correlative data from the simulation to the same data in chimaeric tissue. This is exemplified by using data from the livers of chimaeric animals (obtained by digital analysis of the sections) to establish the area of individual patches, the number of patches in a given area of tissue and the proportions of the two genotypes in the section (Berkwits & Iannaccone, 1985). Based on this quantitative approach it was possible to establish a relation between the patch size in the actual chimaeric liver and the proportion of the two cell types present. The average patch size of areas of livers that have approximately 50% cells derived from PVG-*RT1*^{a} lineage was $2 \times 10^4\ \mu m^2$ (Table 1). The liver, which in this strain of rat averages $12·9 \times 10^{12}\ \mu m^3$ in volume (determined by displacement, assuming a tissue density of 1·08; West, 1976), contains approximately $6·4 \times 10^6$ patches. Since the average patch size varies with the proportion of the two cell types, the number of patches in a liver also depends on the proportion of the two cell types present in that liver (Table 2). The patches are geometrically complex and there is a high standard error of the mean areas. There is a linear relationship between the proportion of a given cell type and the area of the patches generated by that cell type. In the chimaeric rats presented in this study the average patch area varied from $5300\ \mu m^2$ to $20096\ \mu m^2$ for PVG-*RT1*^{a} patches as the pr for this cell type varied from 0·1 to 0·48. The average patch area of PVG patches varied from $5880\ \mu m^2$ to $33589\ \mu m^2$ as the proportion of this cell type varied from 0·16 to 0·35. The relationship between proportion of the given cell type and the patch area is presented in Fig. 7. The nature of the relationship between patch size and the proportion of the two cell types depended on the type of cell under consideration. As the proportion of one of the two cell types increased, the average patch size of that cell type also

Table 1. *Patch analysis of chimaeric liver*

Animal	Lobe (n)*	% PVG-*RT1*^{a} component†	Number of patches per unit area (genotype)‡	Patch area§ (n)
0906	1 (4)	79·9 ± 6·9	32·9 (c)	110·4 ± 85·7 (125)
	2 (4)	83·8 ± 2·4	39·4 (c)	58·8 ± 15·6 (206)
0909	1 (5)	47·6 ± 5·1	16·3 (a)	200·9 ± 29·5 (121)
	2 (3)	67·9 ± 3·6	16·3 (c)	185·6 ± 18·0 (51)
0911	1 (3)	65·2 ± 1·7	11·8 (c)	335·9 ± 74·8 (30)
	2 (5)	61·2 ± 1·3	11·7 (c)	323·8 ± 90·2 (80)
0912	1 (4)	32·2 ± 2·6	26·1 (a)	105·8 ± 7·2 (155)
	2 (5)	9·6 ± 2·0	19·5 (a)	53·0 ± 17·0 (162)

* n, the number of sections analysed; lobe 1 refers to the left lobe, lobe 2 refers to the median lobe.

† Determined by digitizing histological sections as described in 'Materials and methods'; ± S.E.M.

‡ PVG-*RT1*^{a} is designated 'a'; PVG is designated 'c'; the patch analysis is performed on the minor component of the tissue, as described in 'Results'.

§ Results are expressed as the mean $\mu m^2 \times 10^{-2} \pm$ S.E.M.; n is the number of patches analysed.

Table 2. *Estimated number of patches in chimaeric liver*

Proportion*	Genotype†	Number of patches/liver‡	Genotype§
0·90	c	$2{\cdot}4 \times 10^7$	a
0·80	a	$1{\cdot}2 \times 10^8$	c
0·68	c	$1{\cdot}2 \times 10^7$	a
0·68	a	$7{\cdot}0 \times 10^6$	c
0·65	a	$4{\cdot}0 \times 10^6$	c
0·61	a	$3{\cdot}8 \times 10^6$	c
0·52	c	$6{\cdot}4 \times 10^6$	a

* Proportion, % of the major component of the mosaic tissue determined by digitizing sections as described in 'Materials and methods' divided by 100.

† Genotype of the major component; PVG-*RT1*^{a} is designated 'a', PVG is designated 'c'.

‡ Estimated number of patches per liver is determined by assuming an average volume of 12·92 (mean volume of 14 rat livers of this strain).

§ Genotype of the patches (minor component); PVG-*RT1*^{a} is designated 'a', PVG is designated 'c'.

increased. Moreover, since the number of patches measured also decreased, the standard error of the mean increased. The average patch size of the less prevalent cell type became smaller with less variation from patch to patch (in the case of animals with predominantly PVG-*RT1*^{a} cells $r = -0{\cdot}96$; $P < 0{\cdot}003$, while in the case of animals with predominantly PVG cells $r = -0{\cdot}82$; $P < 0{\cdot}001$). The liver of the rat unlike the mouse retina (Schmidt, Wilkinson & Ponder, 1986) displays many large patches. However, small patches (<50 cells) were present and are detectable using the methods described in this report. The distribution of small patches, both for the individual animals and for the total data set, is shown in Fig. 8. The numbers of small patches are normally distributed although they are less prevalent than large patches.

The relationship between the number of patches per unit area and the proportion of the two cell types is shown in Fig. 7. If PVG-*RT1*^{a} patches are counted there is a straight line relation ($r = 0{\cdot}90$; $P < 0{\cdot}01$) with a shallow slope. As the proportion of PVG-*RT1*^{a} cells increased the number of PVG patches increased rapidly, as a straight line ($r = 0{\cdot}88$; $P < 0{\cdot}001$). That is, the number of patches of the minor type increased rapidly since these patches are isolated as islands in a background sea of cells derived from the major type.

It was not possible to readily outline patches of the major cell type, using the digitizer, once the background lattice was formed. This occurs at a proportion of approx. 0·7 in our model as compared with 0·56 in Whitten's model (Whitten, 1978) and 0·9 in West's model (West, 1975). Whitten's model is based on a three-dimensional hexagonal array rather than a two-dimensional array which might affect the proportion at which the lattice forms. The simulation presented here, since it is generational, provides a more sensitive determination of the critical proportion for lattice formation. Moreover, the computer model can count the number of patches of the major type even when the lattice has formed since it counts following subtraction of the other patch type from the array. This approach also allows for the logical elimination of the adjacency problem. This problem results from the choice of two allowable directions of contact, thus presenting a choice of patch membership for a given cell. If the proportion of type 1 cells is varied from 0·1 to 0·5 (the actual proportions tested were $0{\cdot}10 \pm 0{\cdot}01$, $0{\cdot}17 \pm 0{\cdot}003$, $0{\cdot}31 \pm 0{\cdot}014$, $0{\cdot}38 \pm 0{\cdot}015$ and $0{\cdot}49 \pm 0{\cdot}03$) with the computer model, data are generated that allow the comparison of sections from the chimaeras in which PVG proportions were generated from PVG-*RT1*^{a} proportions below 0·5, with subsequent determinations of the number of PVG-*RT1*^{a} patches per unit

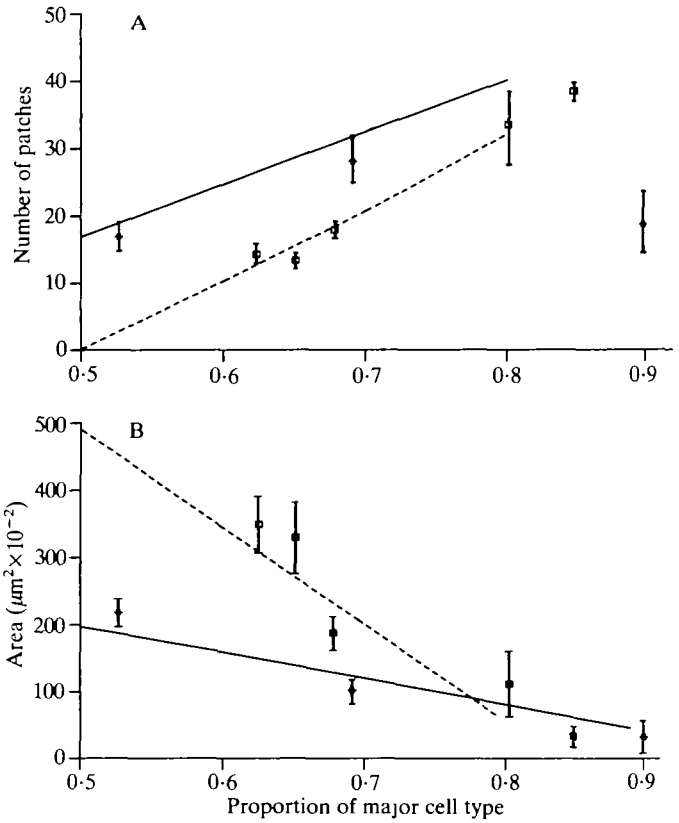

Fig. 7. The relationship between the number of patches (A) and the area of patches (B) of the minor type per unit area of chimaeric tissue and the proportion of the major cell type. The dashed line (▯) represents the number of PVG patches, with increasing proportion of PVG-*RT1*^{a} cells in the tissue. The solid line (•) represents the number of PVG-*RT1*^{a} patches, with increasing proportion of PVG cells in the tissue. The data are presented in this manner since the major cell type formed a background lattice and hence it is the minor cell component which was digitized, as described in 'Results'. The lines represent linear regression of all data between proportion 0·5 and 0·8, the points represent the mean values of all sections from a given liver lobe of each chimaera. Standard errors of the means are presented as vertical bars.

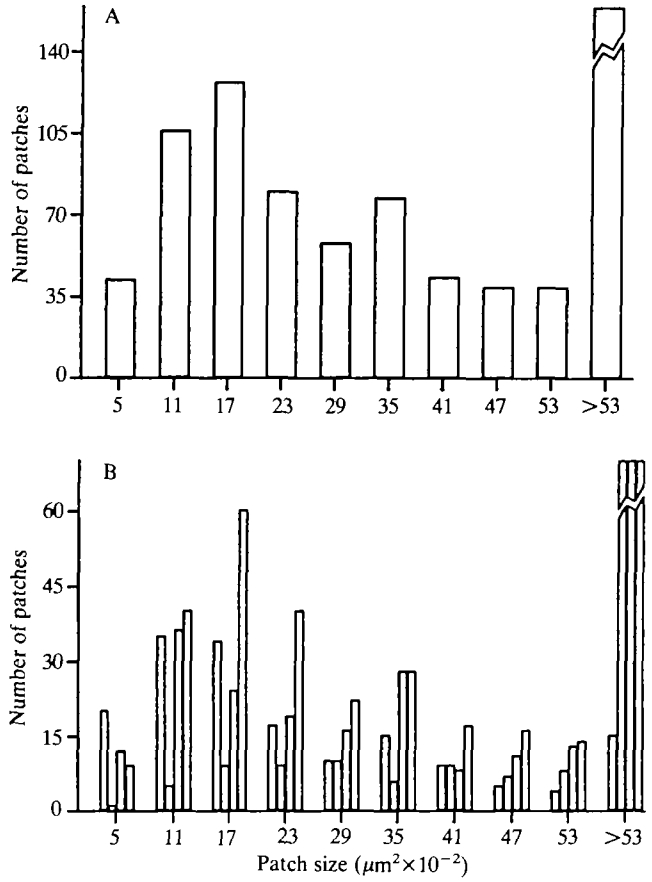

Fig. 8. Histogram representing the distribution of small patches (<50 cells) in the entire data set (A) and each animal individually (B).

area. The computer-generated data were then presented as in Fig. 7 where the data (patch area and number of patches/unit area) for both the PVG-*RT1*^{a} and PVG patches are shown. Again the correlations generated by the simulation are similar to those from the chimaeric liver. The relationship between the simulated number of regions and the proportion of type 2 cells is linear with a positive slope ($r = 0{\cdot}99$; $P < 0{\cdot}001$). The relationship between the areas of these patches and the proportion of type 2 cells is linear with a negative slope ($r = -0{\cdot}90$; $P < 0{\cdot}01$). This analysis is presented in Fig. 9.

As the proportion of the minor cell type decreases, the number of patches cannot increase continuously. At some point there are too few cells of the minor type to support an increasing number of small patches. As the proportion of the minor cell type decreases from this point the number of patches per unit area decreases. This proportion appears to be between 0·8 and 0·9 (0·1 of the minor type) in the computer simulation. The same phenomenon occurs in the chimaeric tissue (Figs 6, 7).

In aggregate the results suggest that the assumptions used to create this model simulation of the generation of a two-dimensional mosaic tissue is adequate, at least to a first approximation, to explain the development of mosaicism in the chimaeric tissue examined. The simulation has demonstrated that complex, finely variegated mosaic patterns can be generated from reiterated simple decisions (the random placement of the two cell types in the anlage, the random order of cell division in each generation and the random choice of adjacent position of the daughter cell). The quantitative analysis of the results of the simulation is in general agreement with the same analysis of chimaeric tissue.

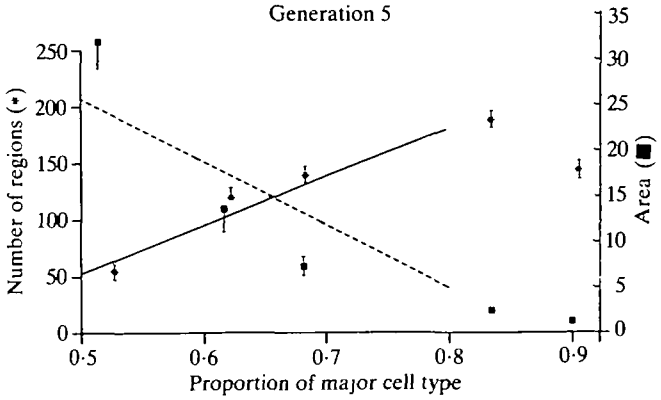

Fig. 9. The results from an additional simulation (combined results of three independent runs as described in 'Materials and methods') are presented to allow comparison of sections from the chimaeras in which PVG proportions were greater than 0·5. In this simulation the proportion of type 1 cells was varied from 0·1 to 0·5. The results are displayed with the proportion of the major cell type (type 2 cells) as the independent variable. The results are presented to demonstrate that the correlations are not biased by which proportions are chosen to start the simulation. The correlation between the area (broken line; ■) of type 1 regions in the computer-simulated mosaic tissue and the proportion of type 2 'cells' in the 'tissue' at generation 5. In this correlation the type 1 regions represent the minor component. The correlation between the number (solid line; •) of type 1 regions per unit area of computer-simulated mosaic tissue and the proportion of type 2 'cells' in the 'tissue' at generation 5 is presented. In this correlation the type 1 regions represent the minor component and, as in the liver from chimaeric animals, the number of regions increases rapidly with increasing proportion of the major 'cell' type, up to pr = 0·8. Standard errors of the means are presented as vertical bars representing values displayed on the appropriate scale (on graph) unless the S.E.M. bar is smaller than the symbol representing the mean.

Discussion

The computer simulation of the development of the mosaic liver clearly establishes that complex, highly variegated mosaicism can be the result of very simple decisions and does not require extensive cell migration. Although there are other computer simulations of mosaic tissue (Whitten, 1978; West, 1975), this is the first that utilizes generational development. The model allows the first attempt at a quantitative analysis of the development of a mosaic tissue. It has been previously held that a fine pattern of mosaicism indicates that cell migration was occurring late into the organogenesis of the organ and that this was responsible for the fine patchiness. Indeed, the liver was considered to be an excellent example of this process. It was thought possible to determine when in the development of the organ cell migration ceased by determining the size of the coherent clone and the patch. The data presented here suggest that only simple probabilistic decisions, not involving cell migration, are required to generate fine patchiness in the liver.

The development of the embryonic liver has been studied since the first half of the 19th century. A large body of published information tends to support the view that the liver is formed by the concurrent development of the endodermal hepatic primordium, which appears as a thickening on the ventral surface of the foregut, and the vascular network which develops from the umbilical vein. The hepatoblastic epithelium develops, not as well-formed cords, but rather as irregular masses of loosely connected cells growing within mesenchyme. These masses of tissue eventually form a single continuous plate, the *muralium simplex*. The embryonic organ is generally considered to be highly plastic and grows rapidly, filling available space (Du Bois, 1963).

At this time there are two prevailing views of the adult liver, one based on a functional anatomy, in which the fundamental unit of the liver is considered the acinus (Rappaport, 1958; Rappaport, MacPhee, Fisher & Phillips, 1983), and the other, based on structural anatomy, in which the fundamental unit of study is the liver lobule (Arey, 1932; Wunsche, 1985; Beketova & Sekamova, 1983). This report has demonstrated that in embryological terms the organogenesis may serve a purpose unrelated to either acinar or lobular development. The pattern of mosaicism described quantitatively in this study in chimaeric animals appears random in the liver and bears no relationship to either the liver zones or the portal structure of the organ.

The liver forms very rapidly in mammalian development and may have purposes in fetal life that are distinct from those in adult life (e.g. haematopoiesis). A number of enzymes important to the adult functions of the organ are not expressed in the liver until after birth, while some enzymes (e.g. γ-glutamyl transpeptidase) that may be important to fetal functions cease to be expressed in the adult liver (Jones & Rolph, 1985; Iannaccone & Koizumi, 1983). As a result it seemed reasonable to test the hypothesis that rapid, probabilistic expansion of tissue with cells occupying fixed positions was all that was required to describe the mosaicism observed in the adult organ. It would appear from the results of this study that a few simple but highly reiterated decisions could be sufficient to place epithelial cells in positions that result in the patterns seen in real tissue.

These conclusions concerning the liver are not generally applicable to other organs. In the adrenal cortex (Weinberg *et al.* 1985*b*) and in intestinal crypts (Schmidt, Wilkinson & Ponder, 1985), for example,

there is clear evidence of clonal development. The correlation between the proportions of cell types and the number of patches/unit area or the average patch area are not correlated in the adrenal gland as they are in the liver and the corresponding computer simulation. This form of modelling in conjuction with pattern analysis of mosaic tissues using histological markers should continue to provide insight to organogenesis in the rat.

This work was supported in part by USPHS grants CA29078 and ES03498 from the DHHS as well as Reproductive Hazards in the Workplace grant 15-49 from the MOD.

References

AREY, L. B. (1932). On the presence of the so-called portal lobules in the seal's liver. *Anat. Record.* **51**, 315.

BEKETOVA, T. P. & SEKAMOVA, S. M. (1983). Sinusoidal cells of the liver and their role in pathologic processes. *Arkh. Patol.* **45**, 83–88.

BERKWITS, L. & IANNACCONE, P. M. (1985). A microcomputer-based quantitative morphometric analysis system for computing areas of amorphous patches. *Comp. Biomed. Res.* **18**, 278–286.

BRUNING, J. L. & KINTZ, B. L. (1968). *Computational Handbook of Statistics*, pp. 152–157. Glenview, Illinois: Scott, Foresman and Co.

DU BOIS, A. M. (1963). The embryonic liver. In *The Liver* (ed. Ch. Rouiller), pp. 1–39. New York: Academic Press.

HUTCHISON, T. H. (1973). A model for estimating the extent of variegation in mosaic tissues. *J. theor. Biol.* **38**, 61–79.

IANNACCONE, P. M. (1980). Clone and patch size in chimeric mouse skin. *Math. Biosci.* **51**, 117–123.

IANNACCONE, P. M. & KOIZUMI, J. (1983). Pattern and rate of disappearance of gamma-glutamyl transpeptidase activity in fetal and neonatal rat liver. *J. Histochem. Cytochem.* **31**, 1312–1316.

JONES, C. T. & ROLPH, T. P. (1985). Metabolism during fetal life: a functional assessment of metabolic development. *Physiol. Rev.* **65**, 357–430.

LEWIS, J. (1973). The theory of clonal mixing during growth. *J. theor. Biol.* **39**, 47–54.

NICOLSON, G. L., YANAGIMACHI, R. & YANAGIMACHI, H. (1975). Ultrastructural localization of lectin binding site on the zonae pellucidae and plasma membranes of mammalian eggs. *J. Cell Biol.* **66**, 263–274.

PAPAIONNOU, V. E. & WEST, J. D. (1981). Relationship between the parental origin of the X chromosomes, embryonic cell lineage and X chromosome expression in mice. *Genet. Res., Camb.* **37**, 183–197.

RAPPAPORT, A. M. (1958). The structural and functional unit in the human liver (liver acinus). *Anat. Record.* **130**, 673–690.

RAPPAPORT, A. M., MACPHEE, P. J., FISHER, M. M. & PHILLIPS, M. J. (1983). The scarring of the liver acini (Cirrhosis). Tridimensional and microcirculatory considerations. *Virchows Arch. [A].* **402**, 107–137.

ROSENFELD, A. & KAK, A. C. (1976). *Digital Picture Processing*, pp. 347–349. New York: Academic Press.

SCHMIDT, G. H., WILKINSON, M. M. & PONDER, B. A. J. (1985). Detection and characterization of spatial pattern in chimaeric tissue. *J. Embryol. exp. Morph.* **88**, 219–230.

SCHMIDT, G. H., WILKINSON, M. M. & PONDER, B. A. J. (1986). Non-random spatial arrangement of clone sizes in chimaeric retinal pigment epithelium. *J. Embryol. exp. Morph.* **91**, 197–208.

WAREHAM, K. A., HOWELL, S., WILLIAMS & WILLIAMS, E. D. (1983). Studies of X-chromosome inactivation with an improved histochemical technique for ornithine carbamoyltransferase. *Histochem. J.* **15**, 363–371.

WEGMANN, T. G. (1970). Enzyme pattern in tetraparental mouse liver. *Nature, Lond.* **225**, 462–463.

WEINBERG, W. C., DEAMANT, F. D. & IANNACCONE, P. M. (1985*a*). Patterns of expression of class I antigens in the tissues of congenic strains of rat. *Hybridoma* **4**, 27–36.

WEINBERG, W. C., HOWARD, J. C. & IANNACCONE, P. M. (1985*b*). Histological demonstration of mosaicism in a series of chimeric rats produced between congenic strains. *Science* **227**, 524–527.

WEST, J. (1975). A theoretical approach to the relation between patch size and clone size in chimaeric tissue. *J. theor. Biol.* **50**, 153–160.

WEST, J. D. (1976). Patches in the livers of chimaeric mice. *J. Embryol. exp. Morph.* **36**, 151–161.

WHITTEN, W. K. (1978). Combinatorial and computer analysis of random mosaics. In *Genetic Mosaics and Chimeras in Mammals* (ed. L. B. Russell), pp. 445–463. New York: Plenum Press.

WUNSCHE, A. (1985). Comparison of liver lobule types, including Rappaport's acinus in swine. *Anat. Histol. Embryol.* **14**, 15–32.

YAMAMURA, K. & MARKERT, C. L. (1981). The production of chimeric rats and their use in the analysis of the hooded pigmentation pattern. *Devl. Genet.* **2**, 131–146.

(Accepted 6 October 1986)